NJC

Accepted Manuscript

ROYAL SOCIETY OF CHEMISTRY

www.rsc.org/njc

Journal Name RSCPublishing

ARTICLE

Cite this: DOI: 10.1039/x0xx00000x

Received 00th January 2012,
Accepted 00th January 2012

DOI: 10.1039/x0xx00000x

www.rsc.org/

Synthesis, Characterization and Field-Effect Transistor Performance of Benzoannulated Pentathienoacene Derivative

Xiangye Qi, [a] Sufen Zou, [ab] Xiaoxia Liu,[ab] Wanglong Hao,[a] Huarong Zhang,[*a] Zhanzhan Zang, [a] Haixia Zhang,[a] Jianhua Gao[*a] and Wenping Hu[*b]

A novel benzoannulated pentathienoacene derivative dihexyl-[1]benzothieno[2'',3'':4',5']thieno[2'',3'':4,5;5'',4'':4',5']bisthieno[3,2-*b*:3',2'-*b*'][1]benzothiophene was designed and synthesized. UV-vis spectra, electrochemistry and thermogravimetric analysis results reveal that this material has large energy bandgap, low-lying highest occupied molecular orbital level and good thermal stability. Atomic force microscopy demonstrates that thin films with high surface roughness and consisted of interconnected sheet-like crystalline grains. A highly ordered aggregation structure in grains was evidenced by X-Ray diffraction measurements. Mobility up to 0.04 cm^{2}v^{-1}s^{-1} and on/off ratio over 10^5 were achieved for the thin film field-effect transistors. These results suggest that this new benzoannulated pentathienoacene derivative is an important member of thienoacene family and will contribute to comprehensive analysis of the structure-property relationships of the thienoacene analogue.

Introduction

Linearly fused π-conjugated systems are significant component as semiconductor material for organic field-effect transistors (OFETs) due to their rigid, coplanar π-conjugated frameworks and unique electronic structures.[1-6] Among all the organic π-conjugated materials, pentacene has been considered as the benchmark semiconductor material for OFETs due to its high charge carrier mobility comparable to amorphous silicon.[7-9] However, pentacene is unstable and degradates rapidly in ambient conditions due to the inherent quinoidal structures which readily undergo photo-induced decomposition and/or thermal oxidation.[10-12] The larger acenes such as hexacene and heptacene exhibit much worse stability.[13-15] As the thiophene analogues of acenes, oligothienoacenes which fully fused oligothiophenes exhibit higher environmental stability and better molecular packing structure.[16-18] Moreover, all the sulfur atoms positioned at the molecular periphery, the intermolecular sulfur–sulfur interaction would increase the effective dimensionality of the electronic structure which facilitates carrier transport.

Thienoacene derivatives, especially benzoannulated oligothienoacenes derivatives, exhibit excellent comprehensive performance such as high mobility and stability due to their integrated advantages of acenes and oligothienoacenes. Scheme 1 lists the model compounds of thienoacene in which the center fused thiophene number varies from one to five. The smallest thienoacene structure DBT, is an important building block for construction of organic semiconductor materials, although no OFETs performance was reported for the DBT molecule itself.[19-20] The alkylated BTBT derivatives exhibit high OFETs performance with mobility higher than 1.0 cm^{2}V^{-1}s^{-1} based on the thin film devices.[21,22] As the combined analogue of pentacene and pentathienoacene, the DBTDT shows higher stability than that of pentathienoacene and pretty good OFETs performance with the thin film mobility[23] of 0.5 cm^{2}V^{-1}s^{-1} and single crystal mobility[24] of 1.8 cm^{2}V^{-1}s^{-1}. The dihexyl-substituted DBTDT exhibits extra high mobility up to 8.8 cm^{2}V^{-1}s^{-1} based on the vacuum deposited thin film devices.[25] However, relatively lower mobility only of 0.15 cm^{2}V^{-1}s^{-1} and 0.48 cm^{2}V^{-1}s^{-1} were obtained for DBTTA[26] and dihexyl-substituted DBTTA[27] thin film transistors respectively,

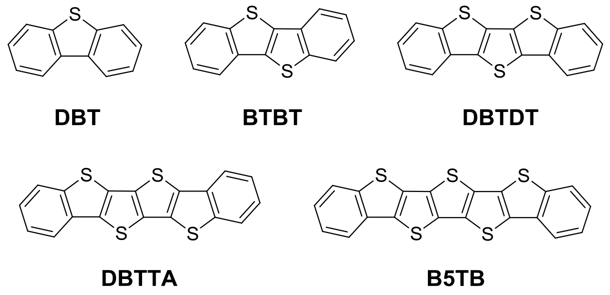

Scheme 1 Model compounds of benzoannulated oligothienoacenes derivatives.

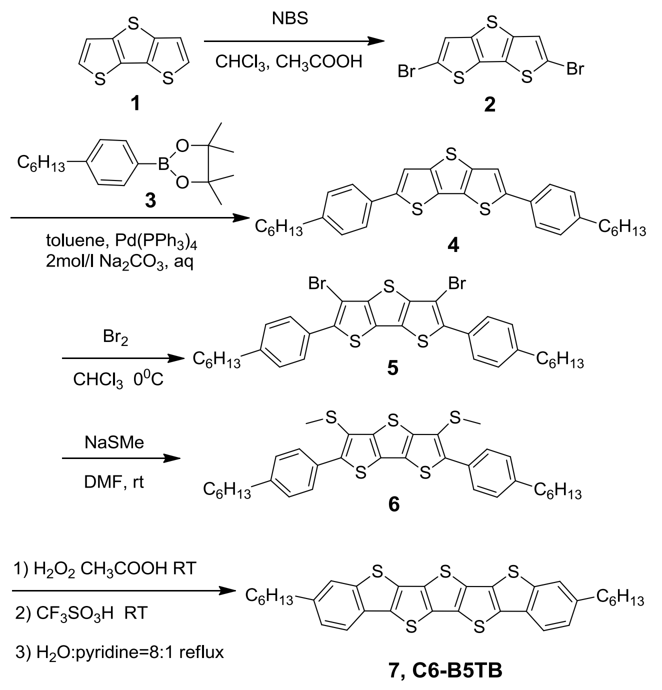

Scheme 2 Synthetic route of **C6-B5TB**.

although with the extended conjugated length. For the benzoannulated pentathienoacene B5TB, the maximum mobility reaches 0.5 $cm^2V^{-1}s^{-1}$ for the crystal transistors,[28] while the alkylated B5TB derivatives have not been reported as far. To analysis the effects of increasing extension of the conjugation and the alkyl substitutes on the charge-transfer properties of organic semiconductors systematically, a dihexyl-substituted B5TB was designed and synthesized in this paper. The physical and chemical properities as well as the thin film transistor performance were also investigated. These results will contribute to a comprehensive understanding of structure-property relationships of such important class of thienoacene derivatives, which is facilitated to design new materials with desired performance.

Results and Discussion

Synthesis of the C6-B5TB

The synthesis approach of compound **C6-B5TB** is illustrated in Scheme 2. Precursor **2**[29] and **3**[30] were obtained by following the known procedure described in the literature. The Suzuki cross-coupling reaction between **2** and **3** afforded compound **4** in moderate yield. After bromination by bromide directively, the dibromide compound **5** was reacted with sodium thiomethoxide to give the cyclization precursor **6**. The compound **6** was oxidized with 30% aqueous hydrogen peroxide in acetic acid, and the intramolecular ring-closing condensation of the methylsulfinyl thiophene with the adjacent phenyl ring proceeded slowly in trifluoromethanesulfonic acid for 24 hours. The final demethylation is achieved by refluxing the suspension in water-pyridine for 10 h to give the target product **7** with a yield of 63%. The alkyl substituents do not increase the solubility of this material distinctly, so the crude compound can be purified easily by washing with normal solvent. The pure product **7** was obtained as a yellow solid after sublimation in a tube furnace.

Optical, electrochemical and thermal properties

The UV-vis absorption spectra of **C6-B5TB** (Fig. 1) in CH_2Cl_2 solution and thin film vacuum-deposited on quartz display strong absorbance in the high energy range. Three main absorption peaks at 350, 371 and 390 nm were observed in solution and the lowest energy absorption at 390 nm was corresponding to the π-π* transition band which dominated by one electron excitation from HOMO to LUMO level. The corresponding optical energy gap is estimated to be 2.98 eV based on the onset of the lowest energy absorption band. In comparison with the absorption in solution, the π-π* transition absorption peak in the thin film was blue-shifted about 28 nm, which indicated a strong H-aggregation was formed.[31, 32]

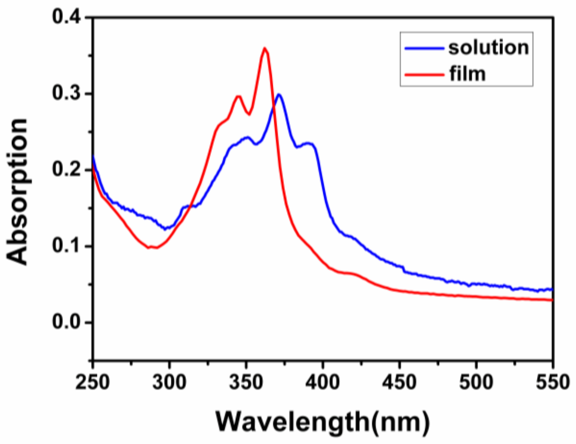

Fig. 1 UV-vis absorption spectra of **C6-B5TB** dilute solution in CH_2Cl_2 and thin film.

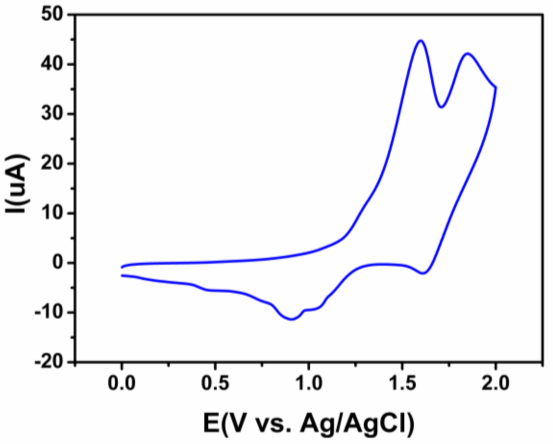

Fig. 2 Cyclic voltammograms of **C6-B5TB**.

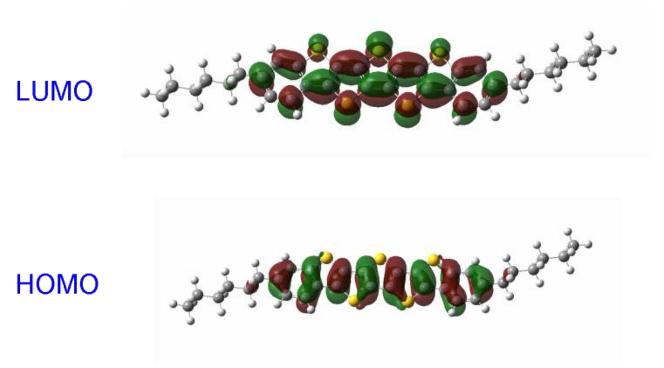

Fig. 3 HOMO and LUMO orbitals of **C6-B5TB** obtained by using DFT calculations.

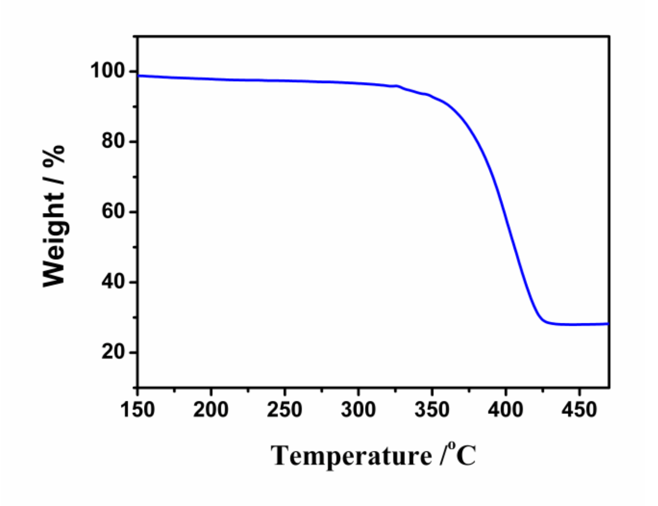

Fig. 4 TGA result of **C6-B5TB**.

Electrochemical characterization was carried out by cyclic voltammetry in CH_2Cl_2 by using ITO as working electrode and Ag/AgCl as reference (Fig. 2). No obvious signal can be observed in the **C6-B5TB** solution due to the low solubility. So the **C6-B5TB** was deposited onto the ITO electrode by thermal evaporation under vacuum before measured. **C6-B5TB** exhibits two quasi-reversible oxidation peaks at E_{pa}=1.59 V and 1.85 V, which demonstrates the good electrical stability of the radical cation. The HOMO energy level estimated from the oxidation onset position (1.14 V) was ca. -5.64 eV.[33] The low-lying HOMO level confirms the enhanced oxidation stability of **C6-B5TB**. To deep explore the electronic structure of the polycyclic aromatic **C6-B5TB**, molecular-orbital (MO) calculations of the HOMO and LUMO levels were performed by using density functional theory (DFT) method at the B3LYP, 6-31G(d,p) level (Fig. 3). The theoretical HOMO (-5.15 eV) level is higher than that estimated by cyclic voltammetry. However, the theoretical bandgap (3.47 eV) predicated from vertical transitions is significantly larger than the optical bandgap nearly 0.5 eV.

The thermal stability of **C6-B5TB** was evaluated by thermogravimetric analysis (TGA) as illustrated in Fig. 4. The TGA result indicates that compound **C6-B5TB** has a good thermal stability and there is no significant mass loss up to 330 ^{o}C (corresponding to a 5 % loss of weight).

Thin films microstructure

The morphology of thin films of **C6-B5TB** prepared on different deposition condition was characterized by atomic force microscope (AFM). As shown in AFM images (Fig 5), thin films exhibited high surface roughness and consisted of interconnected sheet-like crystalline grains. The high roughness has a negative effect on the device performance and the aggregation tendency would result from the strong molecular interaction.

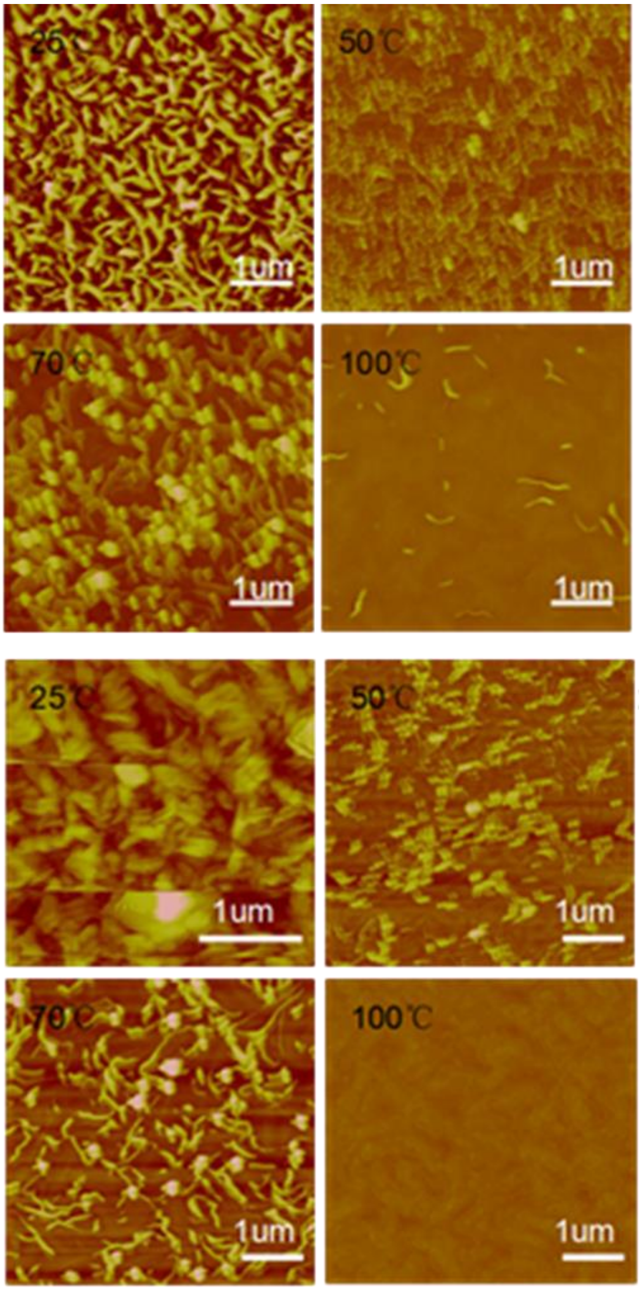

Fig. 5 AFM images of **C6-B5TB** thin films at different substrate temperatures. Up: OTS modified SiO_2/Si substrates; down: SiO_2/Si substrates.

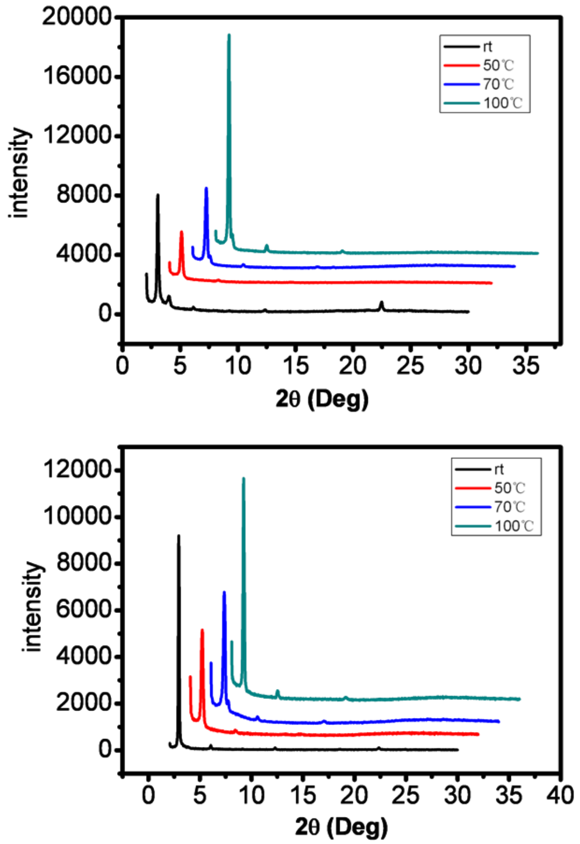

Fig. 6 X-Ray diffraction of **C6-B5TB** film deposited at different substrate temperatures. Up: OTS modified SiO_2/Si substrates; down: SiO_2/Si substrates.

X-ray diffraction (XRD) measurement of **C6-B5TB** thin films deposited on octadecyl-trichlorosilane (OTS) modified and unmodified SiO_2/Si substrates at different temperature showed similar diffraction peaks at $2\theta = 3.2$, 6.5 and 13.0 degree (see Fig. 6), which corresponded to the primary, second and third order diffraction respectively. These results indicate a highly ordered aggregation structure in the deposited films. The primary peak shows strong diffraction and the corresponding d-spacing is ranging in 2.72~2.98 nm due to the flexible hexyl chains, which is very close to the length (about 2.8 nm) of the **C6-B5TB** molecule, which indicates that the molecules are stacked nearly perpendicular to the substrate and formed perfect packing structure, thus facilitating efficient charge carrier hopping transport.

FET device performance

Bottom-gate top-contact OFETs of **C6-B5TB** were fabricated by vacuum deposition on OTS modified and unmodified SiO_2/Si substrates. Au source/drain electrodes were patterned on the organic layer through a shadow mask to afford the devices. FET properties were measured under ambient conditions and all the devices show typical p-type channel field-effect behaviours with hole mobility ranging from 10^{-3} to 10^{-2} $cm^2V^{-1}s^{-1}$. The typical transfer and output curves are shown in Fig. 7 which exhibit well defined field-effect modulations with standard linear and saturation regions. The FET performance obtained at different fabricating conditions is summarized in table 1. It can be seen that the mobility of the OFETs based on bare SiO_2 substrate is slightly higher than that of OTS treated substrate when fabricated at room temperature. However, with the increasing of the substrate temperature, the performances obtained on the OTS treated substrates are all better than those of unmodified substrates. The mobility of **C6-B5TB** increased and a high mobility up to 0.04 $cm^2V^{-1}s^{-1}$ as well as on/off ration over 10^5 was obtained at T_{sub}=70°C on OTS treated substrate. On further increasing the substrate temperature to 100 °C, the mobility decreased slightly. This variation tendency of OFET performance is coincident with the thin film morphology change which revealed by AFM. It is also worth noting that the low threshold voltage (V_{th}) around 10V was observed at all deposition condition. Compared with the less π-extended compounds such as dihexyl-substituted BTBT, DBTDT and DBTTA, the compound **C6-B5TB** showed lower FET performances. This result indicates that the π-conjugated unit is not the more the better. The larger π-extended unit also influence greatly the thin film morphology due to the strong molecular interaction, which in thus affect the carrier migration between the molecules. It is very important to balance the conjugated degrees and intermolecular packing by adjusting the number of conjugated unit in order to obtain superior comprehensive performance.

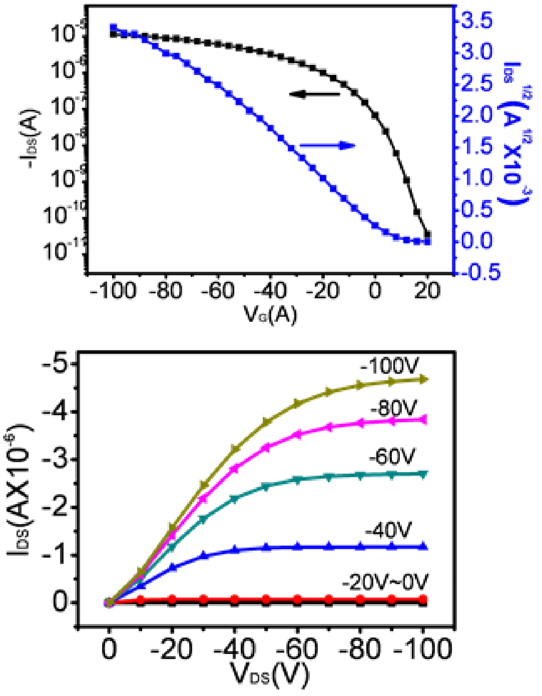

Fig. 7 OFET characteristics of **C6-B5TB** device deposited on the OTS modified substrate at 70 °C. Up: transfer curve in the saturated regime at a constant source-drain voltage of -100 V and square root of the absolute value of the current as a function of the gate voltage. Down: output curves at different gate voltages.

Table 1 OFET characteristics of **C6-B5TB** deposited at different substrate temperature.

T_{sub}	Substrate	Mobility (cm^{2}V^{-1} s^{-1})	V_T (V)	On/off ratio
T=25 ºC	Bare	2.0x10^{-3}	4.9	2x10^2
	OTS	1.56 x10^{-3}	6.8	3x10^2
T=50 ºC	Bare	2.13x10^{-2}	8.4	1x10^5
	OTS	3.80x10^{-2}	7.6	4x10^5
T=70 ºC	Bare	1.76x10^{-2}	12.4	2x10^3
	OTS	3.99x10^{-2}	5.3	3x10^5
T=100ºC	Bare	6.96x10^{-3}	9.3	4x10^3
	OTS	1.18x10^{-2}	-8.0	2x10^5

Conclusions

In conclusion, a novel benzoannulated pentathienoacene derivative **C6-B5TB** is designed and synthesized. UV-vis spectra, electrochemistry and TGA results indicate that this material has large HOMO-LUMO bandgap, low-lying HOMO level and good thermal stability. Mobility up to 0.04 cm^{2}V^{-1}s^{-1} and on/off ratio over 10^5 were achieved for **C6-B5TB** at T_{sub}=70 ˚C on OTS modified substrate. Our preliminary studies demonstrate that dihexylated **C6-B5TB** is a promising candidate for organic semiconductors. Furthermore, these results will contribute to comprehensive analysis of the structure-property relationships of the thienoacene analogue and which would be valuable for the design and development of new organic semiconductors with desired performance.

Experimental Section

Chemicals and instruments

The synthesis procedure of all compounds was depicted in Scheme 2. The dithieno[3,2-b;2′,3′-d]thiophene (**1**)[29] and 2-(4-hexylphenyl)-4,4,5,5-tetramethyl-1,3,2-dioxaborolane (**3**) were synthesized following known literatures. Other reagents and chemicals were obtained from commercial sources and used without further purification. The THF was dried with sodium and distilled before used for reaction solvent. ^{1}H-NMR spectra were recorded on a Bruker DRX-400 and Bruker DRX-300 spectrometer in deuterated chloroform or tetrachloroethane with tetramethylsilane as an internal reference. All chemical shifts were reported relative to tetramethylsilane (TMS) at 0.0 ppm. Elemental analysis was performed by the elementar vario III. The UV-vis spectrum was obtained on a JΛSCO V-570 UV/vis spectrometer. Cyclic voltammeter (CV) was run on a CHI660C electrochemistry station in dichloromethane solution using tetrabutylammonium hexafluorophosphate (Bu_4NPF_6) as electrolyte at a scan rate of 100 mV/s, by using ITO as working electrode, Pt wire as counter electrode. The **C6-B5TB** was deposited onto the ITO electrode by evaporation under vacuum before measured. Thermogravimetric analysis (TGA) was carried out on a Perkin Elmer TGA7.

FET devices were fabricated by the top contact geometry configuration. Thin films were deposited under vacuum onto the OTS modified and unmodified silicon oxide layers. Gold electrodes were deposited by using shadow masks with W/L of ca. 210/27. Organic semiconductors were deposited at a rate of 0.1 Å/s then increasing to 0.4-0.6 Å/s gradually under a pressure of about 2~3×10^{-4} Torr to a final thickness of 50 nm determined by a quartz crystal monitor. OFET characteristics were obtained under ambient atmosphere by Keithley 4200 SCS and Micromanipulator 6150 probe station. X-ray diffraction measurement was performed in reflection mode at 40 kV and 200 mA with Cu Ka radiation using a 2 kW Rigaku D/max-2500 X-ray diffractometer. The films were imaged in air using a Digital Instruments Nanoscope III atomic force microscope operated in tapping mode.

Materials synthesis

2,6-Dibromodithieno[3,2-*b*:2',3'-*d*]thiophene 2: To a solution of dithieno[3,2-b:2',3'-d]thiophene (1.96 g, 10 mmol) in chloroform and acetic acid mixture (25 mL, 1:1) was added NBS（4.45 g, 25 mmol) slowly. After stirred for 24 hours at room temperature, the mixture was extracted with dichloromethane. The organic layer was separated and washed with brine and water respectively, and dried over anhydrous magnesium sulfate. The solvent was removed under reduced pressure, and the residue was purified with column chromatography on silica gel by using petroleum ether as eluent, giving **2** as a white solid. Yield 2.65 g (74.9%). MS m/z: 352. ^{1}H NMR (400Hz, $CDCl_3$): δ7.28 (s, 2H).

2,6-Bis(4-hexyl-phenyl)-dithieno[3,2-*b*;2',3'-*d*]thiophene 4: Compound **2**（0.71 g, 2 mmol), **3** (1.30 g, 4.5 mmol) and $Pd(PPh_3)_4$（0.1 g) were added to 40 mL toluene under nitrogen. After a aqueous Na_2CO_3 solution（15 ml, 2 molL^{-1}) was added, the mixture was refluxed at 110 ˚C for 48 h. The aqueous phase was extracted with CH_2Cl_2, and then the combined organic phase was washed with water and dried over anhydrous magnesium sulfate. The solvent was removed under reduced pressure, and the residue was purified with column chromatography on silica gel by using petroleum ether as eluent to afford **4** as a yellow solid. Yield 0.47 g (48.5%). MS (MALDI-TOF): 516. ^{1}H NMR (400 Hz, $CDCl_3$): δ 7.56 (d, 4H), 7.47 (s, 2H), 7.23 (d, 4H), 2.64 (t, 4H), 1.60-1.67 (m, 4H), 1.32-1.38 (m, 12H), 0.89 (t, 6H).

3,5-Dibromo-2,6-bis(4-hexyl-phenyl)-dithieno[3,2-*b*;2',3'-*d*]thiophene 5: In a round bottom flask immersed in an ice-water bath, compound **4** (0.46 g, 1 mmol) was dissolved in 30 mL chloroform. Bromine (1.1 mL, 2.3 mmol) was added slowly and the mixture was stirred for 12 h. The reaction mixture was then poured into aqueous NaOH solution and extracted with CH_2Cl_2. The organic phase was separated and washed with water and brine respectively, and dried over anhydrous magnesium sulfate. After removal of the solvent, the residue was purified with column chromatography on silica gel by using petroleum ether as eluent. The product **5** was obtained as a yellow solid. Yield 0.5 g (74%). MS (EI) m/z: 676. ^{1}H NMR (400 Hz, $CDCl_3$): δ 7.65 (d, 4H), 7.29 (d, 4H), 2.67 (t, 4H), 1.63-1.70 (m, 4H), 1.32-1.37(m, 12H), 0.90 (t, 6H).

3,5-Bis(methylthio)-2,6-bis(4-hexyl-phenyl)-dithieno[3,2-*b*;2',3'-*d*]thiophene 6: NaSMe (50%, 1 g, 8.3 mmol) was added to a solution of **5** (0.67 g, 1 mmol) in 30 mL DMF. The reaction mixture was stirred for 48 h at room temperature and then poured into saturated aqueous Na_2CO_3 solution. The yellow precipitate formed was filtered and purified with a silica gel chromatographic column by using petroleum ether as eluent to afford compound **6** as a yellow solid. Yield 0.39 g (64 %). MS (MALDI-TOF): 608.4. ^{1}H NMR (400 Hz, $CDCl_3$): δ 7.66 (d, 4H), 7.28 (d, 4H), 2.67 (t, 4H), 2.41 (s, 6H), 1.63-1.70 (m, 4H), 1.32-1.38 (m, 12H), 0.91 (t, 6H).

Dihexyl-[1]benzothieno[2'',3'':4',5']thieno[2'',3'':4,5;5'',4'':4',5'] bisthieno[3,2-*b*:3',2'-*b*'][1]benzothiophene (C6-B5TB) 7: A mixture of compound **6** (0.35 g, 0.58 mmol) in 60 mL acetic acid was stirred. To it was added slowly H_2O_2 (30%, 131 mg, 1.28 mmol), and the suspension was dissolved gradually. A yellow solid was obtained after distillation of solvent under reduced pressure. Then the solid was added to 12 mL trifluoromethanesulfonic acid successively. The reaction mixture quickly turned purple and was stirred for 24 h at room temperature. Then water-pyridine (135 mL, 8:1) was added, and the suspension was refluxed for 10 h. The resulting solution was treated with CH_2Cl_2 and the precipitation was filtered. After washed with water and dichloromethane, the filtrate was sublimated and the pure product **7** was obtained as a yellow solid. Yield 0.21 g (62.9 %). MS (MALDI-TOF): 580.8. ^{1}H NMR (300Hz, 370K, $C_2D_2Cl_4$): δ 7.60 (d, 4H), 7.18 (s, 2H), 2.67 (t, 4H), 1.64 (m, 4H), 1.26 (m, 8H), 0.80 (m, 6H). Anal.calcd for $C_{32}H_{32}S_5$: C, 66.62; H, 5.59; S 27.79. Found: C, 66.13; H, 5.75; S, 27.83.

Acknowledgements

The authors acknowledge financial support from National Natural Science Foundation of China (51003022, 21272049), the Ministry of Science and Technology of China (2013CB933500). Xiangye Qi and Sufen Zou contributed equally to this work.

Notes and references

a Key Laboratory of Organosilicon Chemistry and Material Technology of Ministry of Education, Hangzhou Normal University, Hangzhou 311121, P.R.China. Fax: +86-571-28865135; Tel: +86-571-28865135; E-mail:gaojh@hznu.edu.cn, zhanghuaxy99@hznu.edu.cn
b Key Laboratory of Organic Solids, Institute of Chemistry, Chinese Academy of Sciences, Beijing 100190, P. R. China. Tel: +86-10-82615030; huwp@iccas.ac.cn

Electronic Supplementary Information (ESI) available: See DOI:10.1039/b000000x/

1 J. Mei, Y. Diao, A. L. Appleton, L. Fang and Z. Bao, *J. Am. Chem. Soc.*, 2013, **135**, 6724−6746.

2 W. Wu, Y. Liu and D. Zhu, *Chem. Soc. Rev.*, 2010, **39**, 1489-1502.

3 U. Scherf, *J. Mater. Chem.*, 1999, **9**, 1853-1864.

4 C. Wang, H. Dong, W. Hu, Y. Liu and D. Zhu, *Chem. Rev.*, 2012, **112**, 2208-2267.

5 C. D. Dimitrakopolous and P. Malenfant, *Adv. Mater.*, 2002, **14**, 99-117.

6 Y. Wen, Y. Liu, Y. Guo, G. Yu and W. Hu, *Chem. Rev.*, 2011, **111**, 3358-3406.

7 L. B. Roberson, J. Kowalik, L. M. Tolbert, C. Kloc, R. Zeis, X. Chi, R. Fleming and C. Wilkins, *J. Am. Chem. Soc.*, 2005, **127**, 3069-3075.

8 M. Kitamura and Y. Arakawa, *J Phys Condens Matter*, 2008, **20**, 184011.

9 H. Klauk, M. Halik, U. Zshieschang, G. Schmid, W. Radlik and W. Weber, *J. Appl. Phys.*, 2002, **92**, 52-59.

10 A. Maliakal, K. Raghavachari, H. Katz, E. Chandross and T. Siegrist, *Chem. Mater.*, 2004, **16**, 4980-4986.

11 R. Reddy and M. Bendikov, *Chem. Commun.*, 2006, **11**, 79 –81.

12 P. Coppo and S. G. Yeates, *Adv. Mater.*, 2005, **17**, 3001-3005.

13 J. E. Anthony, *Angew. Chem.*, 2008, **120**, 460-492.

14 S. S. Zade and M. Bendikov, Angew. C*hem. Int. Ed.*, 2010, **49**, 4012-4015.

15 C. Tönshoff and H. F. Bettinger, *Angew. Chem. Int. Ed.*, 2010, **49**, 4125-4128.

16 K. Xiao, Y. Liu, T. Qi, W. Zhang, F. Wang, J. Gao, W. Qiu, Y. Ma, G. Cui, S. Chen, X. Zhan, G. Yu, J. Qin, W. Hu and D. Zhu, *J. Am. Chem. Soc.*, 2005, **127**, 13281-13286.

17 Y. Liu, X. Sun, C. Di, Y. Liu, C. Du, K. Lu, S. Ye and G. Yu, *Chem. Asian J.*, 2010, **5**, 1550-1554.

18 X. Zhang, A. P. Cote and A. J. Matzger, *J. Am. Chem. Soc.*, 2005, **127**, 10502-10503.

19 J. Gao, L. Li, Q. Meng, R. Li, H. Jiang, H. Li and W. Hu, *J. Mater. Chem.*, 2007, **17**, 1421-1426.

20 C. Wang, Z. Wei, Q. Meng, H. Zhao, W. Xu, H. Li and W. Hu, *Org. Electron.*, 2010, **11**, 544-551.

21 H. Ebata, T. Izawa, E. Miyazaki, K. Takimiya, M. Ikeda, H. Kuwabara and T. Yui, *J. Am. Chem. Soc.*, 2007, **129**, 15732-15733.

22 A. Y. Amin, A. Khassanov, K. Reuter, T. M. Friedrichsen and M. Halik, *J. Am. Chem. Soc.*, 2012, **134**, 16548-16550.

23 J. Gao, R. Li, L. Li, Q. Meng, H. Jiang, H. Li and W. Hu, *Adv. Mater.*, 2007, **19**, 3008-3011.

24 R. Li, L. Jiang, Q. Meng, J. Gao, H, Li, Q, Tang, M, He, W. Hu, Y. Liu and D. Zhu, *Adv. Mater.*, 2009, **21**, 4492-4495.

25 Y. Miyata, E. Yoshikawa, T. Minari, K. Tsukagoshi and S. Yamaguchi, *J. Mater. Chem.*, 2012, **22**, 7715-7717.

26 J. Huang, H. Luo, L. Wang, Y. Guo, W. Zhang, H. Chen, M. Zhu, Y. Liu and G. Yu, *Org. Lett.*, 2012, **14**, 3300-3303.

27 X. Liu, X. Qi, J. Gao, S. Zou, H. Zhang, W. Hao, Z. Zang, H. Li and W. Hu, *Org. Electron.*, 2014, **15**, 156–161.

28 K. Yamada, T. Okamoto, K. Kudoh, A. Wakamiya, S. Yamaguchi and J. Takeya, *Appl. Phys. Lett.*, 2007, **90**, 072102.

29 G. F. Pedulli, M. Tiecco, M. Guerra, G. Martelli and P. Zanirato, *J. Chem. Soc. Perkin. Trans.*, 1978, **2**, 212-217.

30 M. Sonntag and P. Strohriegl, *Tetra. Lett.*, 2006, **47**, 8313-8317.

31 S. Hotta, Y. Ichino, Y. Yoshida and M. Yoshida, *J. Phys. Chem. B*, 2000, **104**, 10316-10320.

32 M. S. Kim, E. H. Cho, D. H. Park, H. Jung, J. Bang and J. Joo, *Nanoscale Res. Lett.*, 2011, **6**, 405-412.

33 M. Thelakkat and H. W. Schmidt, *Adv. Mater.*, 1998, **10**, 219-223.

Table of Contents

Graphical abstract:

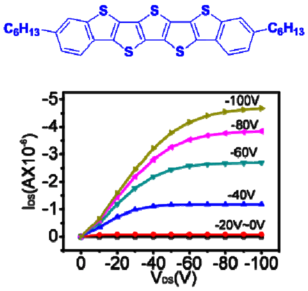

Textual abstract:

New dihexyl-substituted thienoacene derivative exhibits high stability and with a mobility of 0.04 $cm^2v^{-1}s^{-1}$ based on its thin film transistors.